



X-doped Graphene Interaction with Anodic Material LIBs

HAMID REZA JALILIAN, MAJID MONAJJEMI* and HOSSEIN AGHAEI

Department of Chemistry, Science and Research Branch, Islamic Azad University, Tehran, Iran.

*Corresponding author E-mail: m_monajjemi@srbiau.ac.ir

<http://dx.doi.org/10.13005/ojc/330505>

(Received: April 29, 2017; Accepted: June 05, 2017)

ABSTRACT

The structures of graphite carbonadoes and hexagonal boron nitride or h-BN, parent materials for carbonadoes and boron nitride nano-compounds are quite similar. The measured reversible Li⁺ capacities of X-G// (h-BN)// X-G (X=Be, B, N) in the anode materials are extremely improved compared to the graphite structures in the based anodes. In this study Boron nitride sheet has been localized inside two X-graphene electrodes as an option to enhance electrochemical ratio. Additionally, we have found the structure of G-X/(h-BN)_n/X-G can be for improving the capacities and electrical transports in the C-BN sheets of LIBs. In addition, the BN sheet modified and designed of X-G/ (h-BN)/X-G structures provide a strategy to improve the yields of BN-G-sheet of anodes. X-G/h-BN/X-G could also be assembled into free standing electrode of any binder (current collector), which will cause for increasing specific energies and densities for the batteries design.

Keyword: Graphene, Doping, Anode lithium, Ion battery, LIBs.

INTRODUCTION

The carbonaceous materials such as graphite are layered materials composed of hexagonal lattice sheets; graphite^{1,2} is including of carbon atoms at all direction in the lattice points, while the h-BN is consist of alternating atoms from boron and nitrogen respectively. The lattice constants for graphite and h-BN are 2.46 Å and 2.50 Å respectively^{1,2}. In other side, layered BN is transparent and is an insulator^{2,3} compare to graphite. The layers of h-BN are arranged as boron atoms in one layer which are located directly² on the top of nitrogen² atoms in a neighboring section and vice versa³. In graphite

structures, stacking³ is slightly different² while hexagons are offset² and cannot lie on the top of each other so interlayer distances can be consider similar: 3.35 Å for graphite¹ and 3.33 Å for h-BN respectively Figure.1.

Recently, the theoretical approaches have been presented the band structures³ of alone layer of graphite and h-BN while for a layer of graphite which called graphene, 2 bands cross each other at the Fermi³ energies. For this matter, graphene is a semimetal⁴. In contrast graphene, for a layer of the h-BN, equivalent⁴ bands cannot cross each other and amount 4.5 eV band gap forms. Via an

experiment, h-BN has been calculated to have a band gap around 5.8 eV⁴. Crystallographic of BN is classified into four polymorphic³ forms: Hexagonal⁴ BN (h-BN) (Fig 1(a)); rhombohedral^{3,4} BN (r--BN); cubic B-N (c--BN); and wurtzite⁴ BN (w--BN).

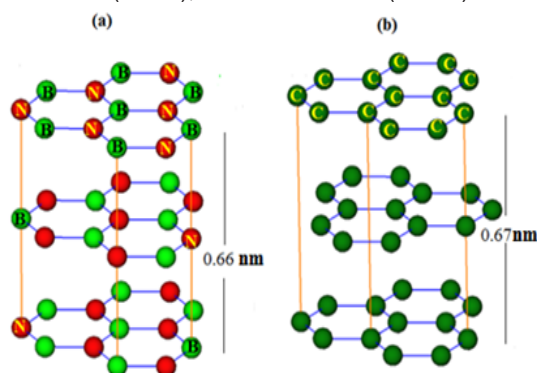


Fig.1. Crystal structures of (a) graphite; (b) hexagonal boron nitride

In 1842, Balmain⁵ sensitized- BN as reaction products via boric-oxide and potassium cyanide⁵ through 1 atmosphere pressure. Then, various methods have been reported through h-BN and r-BN which formed under ambient⁵ pressure and c-BN has been synthesized from h-BN via high pressure and high temperatures. It is notable that w-BN is prepared from h-BN via high pressure at room temperature⁶.

The discovery of amazing reversible, low-voltage⁷ Li-intercalation carbonaceous⁸ materials, Sony Company realized the commercialization⁷ of xC₆/Li_{1-x}CoO₂ cells in 1991⁷. Lithium ion batteries (LIBs) are widely used in small grid storage systems.

LIBs generally consist of positive and negative electrodes including a conducting electrolyte where store electrical energy in the two electrodes⁸ in the form of Li-intercalation⁸ compounds. Electrodes, separator, and electrolyte are the main components of the LIB where the anode plays an essential role in the performance of these devices.

In the charging mechanism of the LIBs, Li⁺ released from the negative electrode and move inside the electrolyte then inserted into the positive electrode. In the discharging mechanism, Li⁺ are extracted⁸ from the (+) electrode and move back to the (-) electrode. Although the electrolyte

establishes high ionic conductivity⁹ between two electrodes, the electrolytes⁹ are not responsible^{8,9} for the conduction of free-electrons. So the electrons complete the 1/2 reaction will move in the way of an extra⁹ external wire.

Various experiments have accomplished for confirming the utilization of graphene in the forms of nano-sheets or nano-ribbons for enhancing lithium storage⁹ capacities and for improving recharge performance⁹⁻¹¹. Furthermore in this study, semi-empirical MM calculations have been done for investigating Li⁺ storage between two graphene¹¹ sheets¹², as well as a few heteroatom-substituted¹¹ carbon materials¹³.

Dis-charging or charging of Li⁺ in carbonadoes is well established and arranged up to now¹⁸⁻²¹. It has also been exhibited the mechanism of the repulsive forces¹³ in the mixed stages which can result in the pure stages during intercalation^{19,23}. In this study, charging and discharging of Li-ions has investigated in h-BN with the positive electrode reaction as: $\text{LiCoO}_2 \rightleftharpoons \text{Li}_{1-x}\text{CoO}_2 + x\text{Li}^+ + x\bar{e}$ and the negative electrode reaction as: $x\text{B}_3\text{N}_3 + x\text{Li}^+ + x\bar{e} \rightleftharpoons \text{LiB}_3\text{N}_3$, while the whole reaction is: $\text{LiCoO}_2 + x\text{B}_3\text{N}_3 \rightleftharpoons \text{Li}_{1-x}\text{CoO}_2 + x\text{LiB}_3\text{N}_3$. It has been suggested²² that lithium atoms are stored²³ via two mechanisms: intercalation and alloying²⁴.

Recently many works has been established for describing the intercalation and diffusion of Li⁺ at different sites on carbonadoes graphite and many studies have been performed in order to explain the mechanism by which Li⁺ are stored in electrodes, including theoretical works¹³⁻²⁴.

The electrical conductivities for the Li⁺-Graphene increases²⁵ via increasing intercalation levels due to the donor²⁶ nature of electrons for the lithium. This is in contrast of ionic conduction²⁶ in which diffusivity²⁷ decreases²⁶ due to the insertion of Li ions²⁷. In the case of amorphous²⁶ carbon as the disorder²⁸ increases electrical conductivity²⁸ significantly decreases²⁹. Recently, Fisher group fabricated²⁹⁻³⁰ a tube-in-tube structure with Li⁺ intercalation capacities² times higher than that of the template-synthesized^{30,40} Carbon-NTs, as the inner tubules provided more electrochemical^{40,43} active sites for intercalation of Li ions^{28,51}.

Boron nitride tubes(BN-NT), which firstly predicted and synthesized by Rubio and Chopra respectively^{40,48}, has a structural similar to Carbon-NTs but, in contrast to the Carbon-NTs being metallic 40(semiconductor) depending on chirality^{42,46}. BNNTs are usually can be an insulator regardless of their helicity, tube diameters and number of tube walls⁴²⁻⁴⁹.

Experimental results have exhibited that small SW-Carbon-NTs are usually found inside multi-walled Carbon-NTs⁴⁰⁻⁵¹. There is, therefore⁴⁹, also a strong motivation to study in detail the stability and interaction of small Boron-Nitride-NTs inside a larger one (viewpoint of diameters), which makes easier to understand the experimental results. Besides, the study on double-walled Boron-Nitride-NTs (DBN-NTs) has demonstrated an interesting variation in their electronic⁵⁰ properties when compared with those of freestanding⁴⁹ component of BNNTs⁴⁸⁻⁵¹. So it is also important to see the inter-wall coupling behavior and interaction energies associated with the small Boron-Nitride-NTs.

In summary, Graphene and h-BN compounds as one kind of classical materials ⁴² with a mature studied history will play a significant role in the battery market of the near future, but how to combine hybrid materials together to obtain safe, stable, and high-capacity electrodes has always been the radical problem that many researchers are trying to solve.

Theoretical background

Diffusion properties^{45,51} of Li ion cell determine some of the key performance metrics of Li⁺ ion batteries cells, consist of the charges and discharges rate, practical capacities and cycling stabilities. The governing equation describing the diffusion process is known as Fick's law as:

$$j_i = -D_i \Delta C_i \quad (1) \quad \text{And} \quad \frac{\sigma_i}{\sigma_t} = \nabla \cdot (D \nabla C_i) \quad (2)$$

where “ j_i ” is ionic flux, mol cm⁻² s⁻¹, D_i is diffusivity of solute ($i = 1, 2$), cm² s⁻¹ and C_i is concentration of species i , (mol cm³). The proportionality⁴⁰⁻⁵⁰ factor D is the diffusivity or diffusion coefficient as

$$D_i = \frac{K_B T}{6\pi\mu R_0} \quad (3)$$

Li⁺ ion cells consist of, all key phenomena involves conducting charged particles

as a primary cell from cathodes to anode or vice versa as a secondary cell from anode to cathodes. Typical commercially used lithium-ion battery consists of several interconnected electrochemical cells, where each cell is composed of a graphite anode (such as Meso-carbon microbeads), a cathode formed by lithium metal oxide (such as LiCoO₂) and electrolyte (such as LiPF₆ dissolved in ethylene carbonate/dimethyl carbonate mixture) embedded in a separator felt.

Anode materials

In the case of anode, Li metal is found to be the most electropositive (-3.04 V versus standard hydrogen electrode) with large reversible capacity ($\approx 4000 \text{ A h kg}^{-1}$). However, due to safety considerations (explosion hazards as a result of dendrite growth during cycling), metallic Li has been substituted by various carbonaceous materials.

During discharge, Li⁺ ions are extracted from the layered graphite, they pass⁵⁵ through the electrolytes and intercalate among the LiCoO₂ layers (Fig.2).

Density and energy of lithium in diffusion model

The electron densities has been defined as ^{52,54}. Where η_i is occupational number of orbitals (i), ϕ are orbitals wave functions, χ is basis function and C is coefficient matrix, the element of i_{th} row j_{th} column⁵² corresponds to the expansion coefficient of orbital j respect to basis function i . Atomic unit for electron density can be explicitly⁵⁴ written as e/Bohr^3 . Electron localization and chemical reactivities⁵⁵ have been built by Bader⁵⁵.

$$\rho(r) = \eta_i |\phi_i(r)|^2 = \sum_i \eta_i \left| \sum_j C_{i,j} \chi_j(r) \right|^2 \quad (5)$$

$$\nabla \rho(r) = \left[\left(\frac{\partial \rho(r)}{\partial x} \right)^2 + \left(\frac{\partial \rho(r)}{\partial y} \right)^2 + \left(\frac{\partial \rho(r)}{\partial z} \right)^2 \right]^{\frac{1}{2}} \quad (6)$$

$$\nabla^2 \rho(r) = \frac{\partial^2 \rho(r)}{\partial x^2} + \frac{\partial^2 \rho(r)}{\partial y^2} + \frac{\partial^2 \rho(r)}{\partial z^2} \quad (7)^{52,54}$$

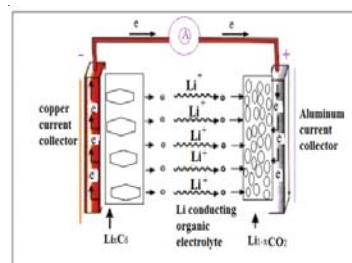


Fig. 2 a typical commercial lithium-ion battery

The Hamiltonian kinetics energies densities K(r)

The kinetic energies densities are not defined, since it has been expected value for kinetic energies operators $\langle \varphi - (\frac{1}{2}) \nabla^2 \varphi \rangle$ (8) has been recovered via integrating kinetic energies densities from an alternative definition. One of general used definition can be demonstrated as:

$k(r) = -\frac{1}{2} \sum_i \eta_i \varphi_i^*(r) \nabla^2 \varphi_i(r)$ (9) "G(r)" is famous as positive definite kinetic energies densities.

$G(r) = \frac{1}{2} \sum_i \eta_i \nabla(\varphi_i^2) = \frac{1}{2} \sum_i \eta_i \left[\left(\frac{\partial \varphi_i(r)}{\partial(x)} \right)^2 + \left(\frac{\partial \varphi_i(r)}{\partial(y)} \right)^2 + \left(\frac{\partial \varphi_i(r)}{\partial(z)} \right)^2 \right]$ (10) K(r) and G(r) are directly related by Laplacian of electron density.

$$\frac{1}{4} \nabla^2 \rho(r) = G(r) - K(r) \quad (11)$$

Electron localization function (ELF)

Becke and Edgecombe noted that spherically averaged likespin conditional pair probability has direct correlation with the Fermi hole and then suggested electron localization function (ELF)⁵³⁻⁵⁴.

$$\text{ELF}(r) = \frac{1}{1 + [D(r)/D_0(r)]^2} \quad (12) \text{ where } D(r) = \frac{1}{2} \sum_i \eta_i \nabla \varphi_i^2 - \frac{1}{8} \left[\frac{\nabla \rho_\alpha^2}{\rho_\alpha(r)} + \frac{\nabla \rho_\beta^2}{\rho_\beta(r)} \right] \quad (13)$$

and $D_0(r) = \frac{3}{10} (6\pi^2)^{\frac{2}{3}} [\rho_\alpha(r)^{\frac{5}{3}} + \rho_\beta(r)^{\frac{5}{3}}]$ (14) for close-shell system, since $\rho_\alpha(r) = \rho_\beta(r) = \frac{1}{2} \rho$ D and D_0 terms can be simplified as $D(r) = \frac{1}{2} \sum_i \eta_i \nabla \varphi_i^2 - \frac{1}{8} \left[\frac{\nabla \rho^2}{\rho(r)} \right]$ (15)

$D_0(r) = \frac{3}{10} (3\pi^2)^{\frac{2}{3}} \rho(r)^{\frac{5}{3}}$ (16) Savin, has reinterpreted the ELF⁵² in the view of kinetics energies⁵²⁻⁵⁸.

$$\text{LOL}(r) = \frac{\tau(r)}{1 + \tau(r)} \quad (17) \text{ where } \tau(r) = \frac{D_0(r)}{\frac{1}{2} \sum_i \eta_i \nabla \varphi_i^2} \quad (18) \quad D_0(r)$$

for spin-polarized system and close-shell system are defined in the same way as in ELF⁵³.

Local Entropies

Local information entropies are quantification of information, which was proposed by Shannon to decompose di-atomic and tri-atomic molecules into space by a minimized information entropy^{52,57}. Parr has discussed the relationship between information entropies and atom partition as well as molecular⁵⁴ similarity⁵⁴. Noorzadeh and Shakerzadeh suggested using information entropy to study aromaticity. probability function is $s = -\int P(\chi) \ln P(\chi) d\chi$ (19). If P(x) is replaced by $\frac{P(r)}{N}$ then the integrand can be called LIE of electrons. $S(r) = -\frac{P(r)}{N}$ in $\frac{P(r)}{N}$ (20) Where, N is the total number of electrons in current system.

At each inter-tube configuration, a single-point calculation is carried out and the total energy is recorded. The resulting sliding-rotation energy

surfaces are used to fix our model in better position. $(E_{\text{total}} - E_{\text{xLi}} + E_{\text{h-BN sheets}}) + E_{\text{BSSE}}$ Where the ΔE_s is the stability energy of system. The contour line map has drawn via Multiwfn software⁵²⁻⁵⁴. The graph sareex habited on interactive interfaces and the methods in this work has based on our previous work⁵⁹⁻⁹⁹.

RESULT AND DISCUSSION

We have listed the data of density, energy, electron localization function (ELF), localized orbital locator (LOL) and local entropy, gap energy, charge from ESP, electrostatic potential, ionization energy, the charges of two doped graphene electrodes and the stability energy of X-G-(h-BN) - X-G and dielectric in 4 tables (tables 1-6) and these data have plotted in 10 the (Figures. 1-10)

We have calculated the gradient norm and the Laplacian of electron density via eqs 7 and 8 for the lithium diffused in the X-G/(h-BN)/X-G system respectively and the data are listed in table 1. For calculation the electron spin density from the difference between alpha and beta density, we have used $p^s(r) = \rho^\alpha(r) - \rho^\beta(r)$ then the spin polarization parameter function will be returned instead of spin density $= \xi(r) = \frac{\rho^\alpha(r) - \rho^\beta(r)}{\rho^\alpha(r) + \rho^\beta(r)}$. The absolute value of going from zero to unity corresponds to the local region going from un-polarized case to completely polarized case Table 1. In this work it has been calculated the local Information entropies for each of Li atoms via eqs. 19-20 and the integrating of those functions over whole spaces yield the information entropies. The data of local Information entropies are listed in Tables 1-5.

Weak interaction (eqs 20 and 21) has significant influence on conformation of macromolecules, however reproduction of electron densities by *ab initio* and grids data calculation of reduced density gradient (RDG) for such huge systems are always too time-consuming. In this work it has been exhibited the complex of X-G/(h-BN)/X-G which demonstrate a high electrical conductivity and a good mechanical strength, excellent flexibility, great chemical stabilities and high specific surfaces area. Those are especially noticeable when the graphene are chemically converted via greater proportion of functional groups, proving that they are suited for using as the base composite

electrodes materials as well as enhancing the electrode's mechanical stabilities. As a result, X-G/(h-BN)/X-G containing electrode materials have high capacity and good rate performance. X-G/(h-BN)/X-G flexibility makes those as an ideal material for buffering metal electrode's volume expansion and contraction

during the charge or discharge phenomenon. Further, the excellent electrical properties of X-G/(h-BN)/X-G can enhance the conductivity of metal electrode material. Finally, the lithium storage capacity for most metal oxide composite materials with X-G/(h-BN)/X-G can be useful greatly.

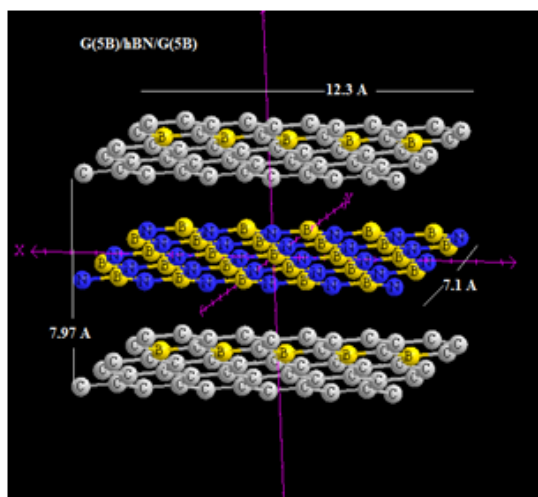


Fig. 3. h-BN sandwich inside two boron graphene doped as two electrodes of B-G/h-BN/B-G and Be-G/h-BN/Be-G capacitors.

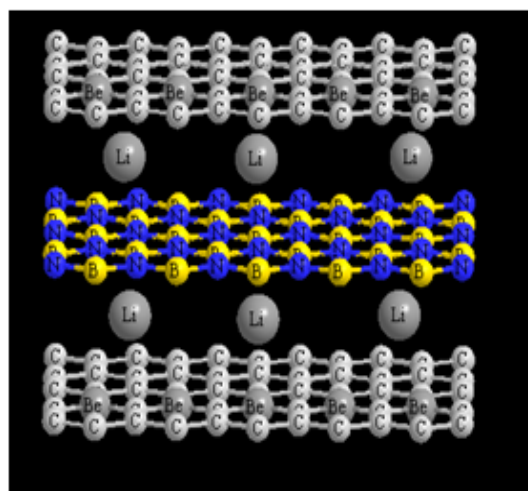


Fig. 4. Six diffused ion lithium between h-BN and B & Be doped graphene sheet layers

Table.1: Density, energy, Electron localization function (ELF), Localized orbital locator (LOL) and Local Entropy for each Li of 6 lithium diffused on X-G/(h-BN)/X-G (X=B,N and Be) mixed layers

Lithium No	Density of all electron $\times 10^{-4}$	Density of α electron (10^{-4})	Density of β electron (10^{-4})	Spin density of electron	Potential energy density $(10^{-3}J)$	Hamiltonian kinetic Energy $(10^{-4}J)$	LOL $\times 10^{-3}$	Local Entropy $\times 10^{-6}$	Ellipticity	ELF 10^{-7}	Eta index	
						x=B						
Li+(2)	0.30	0.15	0.15	0.0	-0.23	-0.15	0.16	0.50	-0.15	0.31	0.16	
Li+(4)	0.26	0.13	0.13	0.0	-0.29	-0.15	0.18	0.52	-0.30	0.32	0.14	
Li+(6)	0.38	0.19	0.19	0.0	-0.27	-0.12	0.17	0.53	-0.22	0.31	0.17	
						X=Be						
Li+(2)	0.22	0.11	0.11	0.0	-0.28	-0.14	0.21	0.50	-0.19	0.38	0.17	
Li+(4)	0.26	0.13	0.13	0.0	-0.27	-0.13	0.18	0.54	-0.12	0.35	0.13	
Li+(6)	0.34	0.17	0.17	0.0	-0.25	-0.15	0.19	0.51	-0.41	0.36	0.16	

Table. 2: The Charges of two doped graphene electrodes and the stability energy of x-G/(h-BN)/x-G.

X= 6 atoms of Be, B and N					
$\text{Li}_x\text{G}-(\text{h-BN})-\text{G}$	$\frac{1}{2}\text{Dielectric thickness(A)}$	$\Delta E_s(\text{ev})=$	$q_{\text{m-G}}^+$	$q_{\text{m-G}}$	$q_{(\text{h-BN})_2}$
X=B					
$\text{Li}_2\text{G}-(\text{h-BN})-\text{G}$	3.98	-14.55	+0.19	-0.15	-0.04
$\text{Li}_4\text{G}-(\text{h-BN})_2-\text{G}$	4.02	-30.32	+0.007	-0.004	-0.003
$\text{Li}_6\text{G}-(\text{h-BN})_2-\text{G}$	3.99	-49.29	+0.14	-0.10	-0.02
X=Be					
$\text{Li}_6\text{G}-(\text{h-BN})_2-\text{G}$	4.03	-33.49	+0.13	-0.010	-0.120

Table. 3: The dielectric of X-G/(h-BN) /X-G modeled in various Lithium number.

$\text{Li}_n\text{X-G}-(\text{h-BN})/\text{X-G}$	$\frac{1}{2}\text{Dielectric thickness(A)}$	$\Delta(V_{\text{B-G}}^{(1)} - V_{\text{B-G}}^{(2)})$	κ
		(a.u.)	
$\text{Li}_2\text{N-G}-(\text{h-BN})/\text{N-G}$	3.97	3.6	1.89
$\text{Li}_2\text{G}-(\text{h-BN})_2-\text{G}$	4.01	2.2	1.83

Table. 4: Nucleor list and HOMO/LUMO and Gap energy for the B-C/h-BN/B-G.

125<C > --> Charge :	4.000000	x,y,z(Bohr):	6.976609	-6.869205	3.400056
126<C > --> Charge :	4.000000	x,y,z(Bohr):	4.651075	-5.976403	4.402859
127 --> Charge :	3.000000	x,y,z(Bohr):	4.651075	-4.190800	6.408467
128<C > --> Charge :	4.000000	x,y,z(Bohr):	6.976610	-3.297999	7.411271
129<C > --> Charge :	4.000000	x,y,z(Bohr):	6.976610	-1.512396	9.416879
130<C > --> Charge :	4.000000	x,y,z(Bohr):	4.651075	-0.619594	10.419683
131<C > --> Charge :	4.000000	x,y,z(Bohr):	2.325540	-12.226014	-2.616768
132<C > --> Charge :	4.000000	x,y,z(Bohr):	0.000005	-11.333212	-1.613964
133<C > --> Charge :	4.000000	x,y,z(Bohr):	0.000005	-9.547609	0.391644
134<C > --> Charge :	4.000000	x,y,z(Bohr):	2.325540	-8.654808	1.394448
135<C > --> Charge :	4.000000	x,y,z(Bohr):	2.325540	-6.869205	3.400056
136<C > --> Charge :	4.000000	x,y,z(Bohr):	0.000005	-5.976403	4.402859
137 --> Charge :	3.000000	x,y,z(Bohr):	0.000005	-4.190800	6.408467
138<C > --> Charge :	4.000000	x,y,z(Bohr):	2.325540	-3.297999	7.411271
139<C > --> Charge :	4.000000	x,y,z(Bohr):	2.325540	-1.512396	9.416879
140<C > --> Charge :	4.000000	x,y,z(Bohr):	0.000005	-0.619594	10.419683
141<C > --> Charge :	4.000000	x,y,z(Bohr):	-2.325549	-12.226014	-2.616768
142<C > --> Charge :	4.000000	x,y,z(Bohr):	-4.651083	-11.333212	-1.613964
143<C > --> Charge :	4.000000	x,y,z(Bohr):	-4.651083	-9.547609	0.391644
144<C > --> Charge :	4.000000	x,y,z(Bohr):	-2.325549	-8.654808	1.394448
145<C > --> Charge :	4.000000	x,y,z(Bohr):	-2.325549	-6.869205	3.400056
146<C > --> Charge :	4.000000	x,y,z(Bohr):	-4.651083	-5.976403	4.402859
147 --> Charge :	3.000000	x,y,z(Bohr):	-4.651083	-4.190800	6.408467
148<C > --> Charge :	4.000000	x,y,z(Bohr):	-2.325548	-3.297999	7.411271
149<C > --> Charge :	4.000000	x,y,z(Bohr):	-2.325548	-1.512396	9.416879
150<C > --> Charge :	4.000000	x,y,z(Bohr):	-4.651083	-0.619594	10.419683
151<C > --> Charge :	4.000000	x,y,z(Bohr):	-6.976618	-12.226014	-2.616768
152<C > --> Charge :	4.000000	x,y,z(Bohr):	-9.302153	-11.333212	-1.613964
153<C > --> Charge :	4.000000	x,y,z(Bohr):	-9.302153	-9.547609	0.391644
154<C > --> Charge :	4.000000	x,y,z(Bohr):	-6.976618	-8.654808	1.394448
155<C > --> Charge :	4.000000	x,y,z(Bohr):	-6.976618	-6.869205	3.400056
156<C > --> Charge :	4.000000	x,y,z(Bohr):	-9.302153	-5.976403	4.402859
157 --> Charge :	3.000000	x,y,z(Bohr):	-9.302153	-4.190800	6.408467
158<C > --> Charge :	4.000000	x,y,z(Bohr):	-6.976618	-3.297999	7.411271
159<C > --> Charge :	4.000000	x,y,z(Bohr):	-6.976618	-1.512396	9.416879
160<C > --> Charge :	4.000000	x,y,z(Bohr):	-9.302153	-0.619594	10.419683
161<C > --> Charge :	4.000000	x,y,z(Bohr):	-11.627688	-12.226014	-2.616767
162<C > --> Charge :	4.000000	x,y,z(Bohr):	-11.627688	-8.654808	1.394448
163<C > --> Charge :	4.000000	x,y,z(Bohr):	-11.627688	-6.869205	3.400056
164<C > --> Charge :	4.000000	x,y,z(Bohr):	-11.627688	-3.297999	7.411271
165<C > --> Charge :	4.000000	x,y,z(Bohr):	-11.627688	-1.512396	9.416879

Note: Orbital 326 is HOMO of alpha spin, orbital 985 is HOMO of beta spin
LUMO/HOMO gap of alpha orbitals: 0.000289 a.u. 0.007873 eV
LUMO/HOMO gap of beta orbitals: 0.000011 a.u. 0.000307 eV

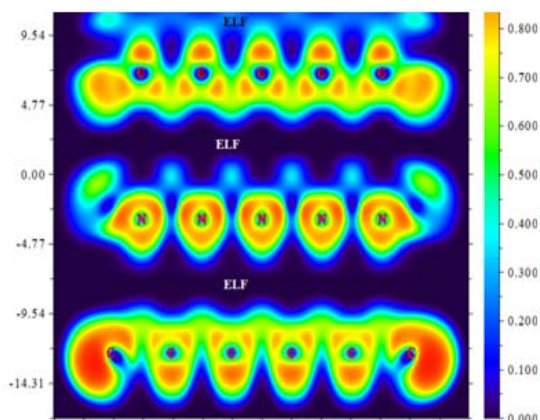


Fig. 5. ELF of B-G/h-BN/B-G for

CONCLUSION

The structure of G-X/(h-BN)_n/X-G can be for improving the capacities and electrical transports in the C-BN sheets of LIBs. In addition, the BN sheet modified and designed of X-G/ (h-BN)/X-G structures provide a strategy to improve the yields of BN-G-sheet of anodes. X-G/h-BN/X-G

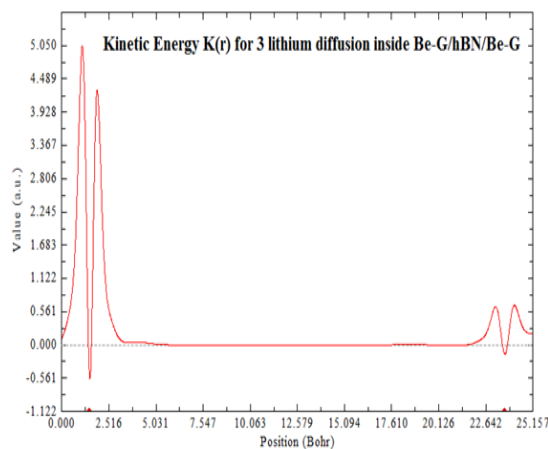


Fig. 6. $K(r)$ of 3 lithium diffusion inside Be-G/h-BN/Be-G

could also be assembled into free standing electrode of any binder (current collector), which will causes for increasing specific energies and densities for the batteries design.

ACKNOWLEDGEMENT

Authors would like to thanks science and research branch of Islamic Azad University, Iran.

REFERENCES

- Tatar, R.C.; Rabii, S. *Physical Review B*. **1982**, 254126-41.
- Sichel, E. K.; Miller, R. E.; Abrahams, M. S.; Buiochi, C. J. *Physical Review B*, **1976**, 13, 4607-11
- Hyun, K.Y.; Chang, K. J.; Louie, S. G. *Physical Review B*, **2001**, 63, 205408 4. A. Zunger, Katzir, A.; Halperin, A. *Physical Review*, **1976**, B 13, 5560-73
- W. H. Balmain, *J. Prakt. Chem.* **1842**, 27, 422
- Sato, T.; *Report of National Institute for Research in Inorganic Materials, Tsukuba, Japan.*, **1987**.
- Yang, Z. G.; Zhang, J. L.; Kintner-Meyer, M. C. W.; Lu, X. C.; Choi, D. W. Lemmon, J. P.; Liu, J.; *Chem. Rev.* **2011**, 111, 3577-3613.
- Guerard, D.; Herold, A.; **1975**, 13, 337-345.
- Yoo, E. J.; Kim, J.; Hosono, E.; Zhou, H. S.; Kudo, T.; *Nano Lett.* **2008**, 8, 2277-2282.
- Wang, G.; Shen, X. P.; Yao, J.; Park, J.; *Carbon*, **2009**, 47, 2049-2053.
- Bhardwaj, T.; Antic, A.; Pavan, B.; Barone, V.; Fahiman, B. D.; *JACS*, **2010**, 132, 12556-12558
- Suzuki, T.; Hasegawa, T.; Mukai, S. R.; Tamon, H.; *Carbon*, **2003**, 41, 1933-1939.
- Hasegawa, T.; Suzuki, T.; Mukai, S. R.; Tamon, H.; *Carbon*, **2004**, 42, 2195-2200.
- Noel, M.; Suryanarayanan, V. *Journal of Power Sources*, **2002**, 111, 193-209.
- Tirado, J.L.; *Materials Science and Engineering R*, **2003**, 40, 103-136.
- Fu, L.J.; Liu, H.; Li, C. Wu, Y.P.; Rahm, E.; Holze, R.; Wu, H.Q. *Solid State Sciences*, **2006**, 8, 113-128
- Frackowiak, E.; Béguin, F.; *Carbon*, **2002**, 40, 1775-1787
- Whittingham, M. S.; Jacobson (Eds.), A.J.; *Intercalation, Chemistry, Academic Press*. **1982**
- Safran, S.A.; Hamann, D.R.; *Physical Review Letters*. **1979**, 42 (21), 1410-1413
- Levi, M.D.; Aurbach, D.; Maier, J. *Journal of*

- Electroanalytical Chemistry*, **2008**, 624 251–261.
21. Zabel, H.; Solin (Eds.), S. A.; *Graphite Intercalation Compound I*, Springer-Verlag, **1990**.
 22. Wu, Y.P.; Rahm, E.; Holze, R. *Journal of Power Sources*, **2003**, *114*, 228–236
 23. Lee, J.K.; An, K.W.; Ju, J.B.; Cho, B.W.; Cho, W.I.; Park, D.; Yun, K.S.; *Carbon*, **2001**, *39*, 1299–1305
 24. C. De las Casas, and W.Z. Li, *J. Power Sources*, **2012**, *208*, 74–85
 25. Z. H. Yang, and H. Q. Wu, *Mater. Chem. Phys.*, **2001**, *71*, 7–11
 26. K.S. Novoselov, A.K. Geim, S.V. Morozov, D. Jiang, Y. Zhang, S.V. Dubonos, I.V. Grigorieva, and A.A. Firsov, *Science*, **2004**, *306*, 666–669
 27. B. Partoens, and F.M. Peeters, *Physical Review B*, **2006**, *74*, 075404-1–075404-11
 28. H. Tachikawa, and A. Shimizu, *Journal of Physical Chemistry B*, **2006**, *110*, 20445–20450
 29. K. Naoi, N. Ogihara, Y. Igarashi, A. Kamakura, Kusachi, K. Utsugi, *Journal of the Electrochemical Society*, **2005**, *152*(6), A1047–A1053.
 30. H. Groult, B. Kaplan, S. Komaba, N. Kumagai, V. Gupta, T. Nakajima, and B. Simon, *Journal of the Electrochemical Society*, **2003**, *150*(2), G67–G75
 31. M. Endo, Y. Nishimura, T. Takahashi, K. Takeuchi, M.S. Dresselhaus, *Journal of Physics and Chemistry of Solids*, **1996**, *57*(6–8), 725–728
 32. T. Ohzuku, R.J. Brodd, *Journal of Power Sources*, **2007**, *174*, 449–456.
 33. Monajjemi, M.; Boggs, J.E.; *J. Phys. Chem. A*, **2013**, *117*, 1670–1684.
 34. Monajjemi, M.; Lee, V.S. Khaleghian, M.; Honarparvar, B.; Mollaamin, F.; *J. Phys. Chem. C*, **2010**, *114*, 15315.
 35. Monajjemi, M.; *Journal of Molecular Modeling*, **2014**, *20*, 2507.
 36. Monajjemi, M. *TheorChemAcc*, **2015**, *134*:77 DOI 10.1007/s00214-015-1668-9.
 37. Monajjemi, M.; *Struct. Chem*, **2012**, *23*, 551
 38. Monajjemi, M.; Jafari Azan, M.; Mollaamin, F. *Fullerenes, Nanotubes, and Carbon Nanostructures*, **2013**, *21*(6), 503–515.
 39. Monajjemi, M.; *Chemical Physics*, **2013**, 425, 29–45
 40. Novoselov, K.S.; Geim, A.K.; Morozov, S.V.; Jiang, D.; Zhang, Y.; Dubonos, S.V.; Grigorieva, I.V. Firsov, A.A. *Science*, **2004**, *306*, 666–669
 41. B. Partoens, and F.M. Peeters, *Physical Review B*, **2006**, *74* 075404-1–075404-11
 42. Monajjemi, M.; Mollaamin, F.; *Journal of Cluster Science*, **2012**, *23*(2), 259–272.
 43. L. Ravagnan, P. Piseri, M. Bruzzi, S. Miglio, G. Bongiorno, A. Baserga, C.S. Casari, A. Li Bassi, C. Lenardi, Y. Yamaguchi, T. Wakabayashi, C.E. Bottani, and P. Milani, *Physical Review Letters*, **2007**, *98*, 216103-1–216103-4
 44. Wu, G.T.; *Journal of Power Sources*, **1998**, *75*, 175
 45. Jalilian, H.; Monajjemi, M.; *Japanese Journal of Applied Physics*, **2015**, *54*, 085101.
 46. Chew, S.Y.; et al., *Carbon*, **2009**, *47*, 2976.
 47. Monajjemi, M.; Khaleghian, M, *Journal of Cluster Science*, **2011**, *22*(4), 673–692
 48. E. Frackowiak, S. Gautier, H. Gaucher, S. Bonnamy, F. Beguin, *Carbon*, **1999**, *37* (1999) 61.
 49. Monajjemi, M.; Wayne Jr, Robert.; Boggs, J.E. *Chemical. Physics*, **2014**, *433*, 1–11
 50. S. Y. Chew, S. H. Ng, J. Wang, P. Novak, F. Krumeich, S. L. Chou, J. Chen, and H. K. Liu. *Carbon*, **2009**, *47*, 2976
 51. E. Frackowiak, S. Gautier, H. Gaucher, S. Bonnamy, and F. Beguin, *Carbon*, **1999**, *37* 61 Joseph, Doninger, Z. Vyacheslav, Barsukov (Eds.), *New Carbon Based Materials for Electrochemical Energy Storage Systems*, Springer, **2006**, 269–276.
 52. T. Lu, F. Chen, *Acta Chim. Sinica*, **2011**, *69*, 2393–2406.
 53. T. Lu, F. Chen, *J. Mol. Graph. Model*, **2012**, (38): 314–323.
 54. T. Lu, F. Chen Multiwfn: A Multifunctional Wavefunction Analyzer, *J. Comp. Chem.* **2012**, (33) 580–592.
 55. R.F.W. Bader, atoms in Molecule: A quantum Theory (Oxford Univ. press, Oxford, **1990**.
 56. Becke and Edgecombe *J. Chem. Phys.*, **1990**, *92*, 5397.
 57. A. Savin, *Angew. Chem. Int. Ed. Engl.*, **1992**, *31*, 187.
 58. J.P. Perdew, K. Burke, Ernzerhof, *Phys. Rev. Lett.* **77**, 3865–3868., **1996**.
 59. Chegini, H.; Mollaamin, F.; Farahani, P. *Fullerenes, Nanotubes, and Carbon Nanostructures*, **2011**, *19*, 469–482
 60. Baei, M.T.; Mollaamin, F. *Russian Journal of Inorganic Chemistry*, **2008**, *53* (9), 1430–1437

61. Mollaamin, F.; Monajjemi, M, *Journal of Computational and Theoretical Nanoscience*. **2012**, *9* (4) 597-601
62. Mollaamin, F.; Varmaghani, Z.; Monajjemi, M, *Physics and Chemistry of Liquids*. **2011**, *49*, 318
63. Razavian, M.H.; Mollaamin,F.; Naderi,F.; Honarparvar,B.; *Russian Journal of Physical Chemistry A* , **2008** , *82* (13), 2277-2285.
64. Monajjemi, M.; Faham, R.; Mollaamin, F. *Fullerenes, Nanotubes, and Carbon Nanostructures*, **2012** *20*, 163–169.
65. Monajjemi, M.; Honarparvar, B. H. ; Haeri, H. ; Heshmat ,M.; *Russian Journal of Physical Chemistry C*. **2006**, *80*(1), S40-S44.
66. Monajjemi, M.; Mollaamin, F. *Journal of Computational and Theoretical Nanoscience*, **2012**, *9* (12), 2208-2214.
67. Monajjemi, M.; Honarparvar, B.; Nasseri, S. M. .; Khaleghian M. *Journal of Structural Chemistry*. **2009**, *50*, 1, 67-77.
68. Ardalan, T.; Ardalan, P.; Monajjemi, M. *Fullerenes, Nanotubes, and Carbon Nanostructures*, **2014**, *22*: 687–708.
69. Monajjemi, M.; Najatpour, J.; Mollaamin, F. *Fullerenes, Nanotubes, and Carbon Nanostructures*. **2013**, *21*(3), 213–232
70. Monajjemi, M. Falahati, M.; Mollaamin, F.; *Ionics*, **2013**, *19*, 155–164
71. Tahan, A.; Monajjemi, M. *Acta Biotheor*, **2011**, *59*, 291–312.
72. Lee, V.S.; Nimmanpipug, P.; Mollaamin, F.; Kungwan, N.; Thanasanvorakun, S.; Monajjemi, M. *Russian Journal of Physical Chemistry A*, **2009**, *83*, 13, 2288–2296.
73. Monajjemi, M.; Heshmat, M.; Haeri, HH, *Biochemistry (Moscow)*, **2006**, *71* (1), S113-S122
74. Monajjemi, M.; Yamola, H.; Mollaamin, F. *Fullerenes, Nanotubes, and Carbon Nanostructures*, **2014**, *22*, 595–603.
75. Monajjemi, M.; Ahmadianarog, M. *Journal of Computational and Theoretical Nanoscience*. **2014**, *11*(6), 1465-1471.
76. Mollaamin, F.; Monajjemi, M. *Physics and Chemistry of Liquids* . **2012**, *50*(5). 596–604.
77. Monajjemi, M.; Khosravi, M.; Honarparvar, B.; Mollaamin, F.; *International Journal of Quantum Chemistry*, **2011**, *111*, 2771–2777
78. Monajjemi, M.; Baheri, H.; Mollaamin, F. *Journal of Structural Chemistry*. **2011**, *52*(1), 54-59
79. Mahdavian, L.; Monajjemi, M.; Mangkomtong, N. *Fullerenes, Nanotubes and Carbon Nanostructures*, **2009**, *17* (5), 484-495
80. Monajjemi, M.; Farahani, N.; Mollaamin, F. *Physics and Chemistry of Liquids*, **2012**, *50*(2) 161–172
81. Monajjemi, M.; Khaleghian, M.; Mollaamin, F. *Molecular Simulation*. **2010**, *36*, 11, 865–
82. Monajjemi, M. *Biophysical Chemistry*. **2015**, *207*, 114 –127
83. Mahdavian, L.; Monajjemi, M. *Microelectronics Journal*. **2010**, *41*(2-3), 142-149.
84. Monajjemi, M.; *Journal of Molecular Liquids*, **2017**, *230*, 461–472.
85. Monajjemi, M.; *Macedonian Journal of Chemistry and Chemical Engineering*, **2017**, *36*, 1, 101–118.